Correction to plasmon spectrum due to dark photons in a graphene periodic structure

Daqing Liu,[1] Dong Sun,[1] Xiuqin Hua,[1] Xingfang Jiang,[1] and Ning Ma[2]
[1]*School of Microelectronics and Control Engineering, Changzhou University, Changzhou 213164, China*
[2]*College of Physics, Taiyuan University of Technology, Taiyuan 030024, China*

(Received 31 August 2023; accepted 17 November 2023; published 13 December 2023)

We proposed a cubic graphene periodic structure as a producer and probe of dark photons in an ordinary-sized laboratory. Utilizing modified Maxwell equations and hydrodynamic model in the system, corrections to dispersions of a collective excitation, plasmon, were demonstrated. If there is kinetic mixing between dark photons and ordinary matter, we found a significant difference in dispersion relationships, specifically a momentum gap in the plasmon dispersion curve. The relation between momentum gap, Compton wave of dark photons, and coupling between dark photon and ordinary photon was obtained. Considering the momentum gap, examining the effect of dark photons in the structure is not difficult.

DOI: 10.1103/PhysRevD.108.123022

I. INTRODUCTION

The dark photon (DP) is a candidate for dark matter and ubiquitous in theories beyond the standard model (SM) since a minimal extension of the SM is a dark photon kinetically mixing with the matters in the SM, such as the ordinary photon [1–3]. They have recently attracted much attention by various experiments/observations and theories [4–12]. Several haloscope experiments, operating at various mass ranges, are currently being conducted worldwide to search for the DP. Most of these experiments/observations were motivated primarily by the search for axions but they are also sensitive to the DP [13–27] in their associated mass range. Since the mass of the DP is unknown, these haloscopes must tune their resonant frequencies to scan for the unknown rest mass. Besides the above experiments, other techniques exist, such as solar radio observations [28] and plasma haloscope experiments [29–31].

In many materials, a collective excited state (plasmon polariton) shares many properties with plasmas. One can also arrange suitable material to produce and detect DP by plasmon in the laboratory. In this paper we proposed a cubic graphene structure to perform the research. We showed that as long as DP can kinetically mix with ordinary matter, dispersion behavior of plasmon in the structure exhibits a significant difference from that without mixing. Specifically, there is a gap in the momentum space for the plasmon dispersion relationship. Since the location of the gap is predictable, even if the mixing is tiny, one can directly use the gap to detect DP-induced effects. Since carriers are confined in graphene materials, the parameters used here, such as layer distance and carrier density (controlled by gate voltage), are simpler to tune in the laboratory than the plasma haloscope method. Additionally, the plasmon temperature can also be controlled by the environment. Thus, the proposed method offers an efficient platform for detecting DP.

II. MODIFIED ELECTROMAGNETISM IN A GRAPHENE STRUCTURE

Suppose a cubic periodic structure of graphene sheets embedded in a medium with permittivity ε (we set ε to be equal to vacuum permittivity ε_0), as shown in Fig. 1. Sizes of graphene sheets are b_1, b_2, and the sides of elementary cell are $b \times b \times d$, which are parallel to the x axis, y axis, and z axis, respectively, and far lower than the wavelength in the medium. The graphene sheet spreads out in the x-y plane in each elementary cell. The coverage ratio of the area of graphene vs the area of the primitive cell in the x-y plane, $b_1 b_2/b^2$, is r. We assume that each graphene layer is N doped and has an equal Fermi energy, $E_F > 0$, with $n_0 = \frac{E_F^2}{\pi\hbar^2 v_F^2}$ where v_F and n_0 are Fermi velocity(1×10^6 m/s) and two-dimensional (2D) carrier equilibrium density, respectively. The effective density of carriers is then $n_3 = \frac{n_0 r}{d} = \frac{r E_F^2}{\pi d \hbar^2 v_F^2}$. From the point of view of effective density, we could absorb the contribution of r into E_F. In the following, we just choose $r \equiv 1$ for simplification, that is, each graphene sheet covers the x-y plane completely.

To derive the modified Maxwell equations with DP in the structure, we first used natural system of units (i.e., we set all the vacuum light speed, Plank constant, vacuum permittivity, vacuum permeability equal to 1, $c = \hbar = \varepsilon_0 = \mu_0 = 1$),

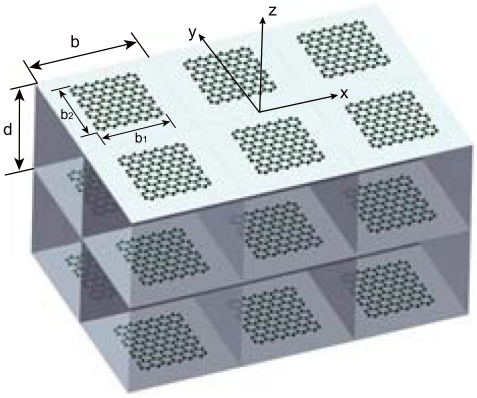

FIG. 1. The cubic periodic structure of graphene sheets embedded in the medium. Sizes of graphene sheets are b_1, b_2, and sides of elementary cell are $b \times b \times d$, which are parallel to the x axis, y axis, and z axis, respectively.

ignoring the boundary conditions for fields provided d is small enough. The Lagrange quantity can be written as [6]

$$\mathcal{L} = \mathcal{L}_1 + \mathcal{L}_2 + \mathcal{L}_3 = -\frac{1}{4}(F^{\mu\nu}F_{\mu\nu} + X^{\mu\nu}X_{\mu\nu}) - J^{\mu}A_{\mu} + \frac{m_X^2}{2}(X^{\mu}X_{\mu} + 2gX^{\mu}A_{\mu}), \tag{1}$$

where A^{μ} and $F^{\mu\nu} = \partial^{\mu}A^{\nu} - \partial^{\nu}A^{\mu}$ (X^{μ} and $X^{\mu\nu} = \partial^{\mu}X^{\nu} - \partial^{\nu}X^{\mu}$) are vector potential and the second order contravariant field strength tensor for photon (dark photon), respectively, J^{μ} is 4D current density, g is the coupling between photon and dark photon, and m_X refers to the mass of dark photons.

Then, according to the Euler-Lagrange equation, we found that

$$\begin{aligned} \partial_{\rho}F^{\rho\sigma} &= J^{\sigma} - gm_X^2X^{\sigma}, \\ \partial_{\rho}X^{\rho\sigma} &= -m_X^2(X^{\sigma} + gA^{\sigma}). \end{aligned} \tag{2}$$

Since DP is massive spin-1 field, it satisfies Lorentz gauge. Furthermore, we took Lorentz gauge for photon field. In other words, we have $\partial_{\rho}X^{\rho} = \partial_{\rho}A^{\rho} = 0$. The equation of motion for DP is as follows:

$$(\partial_0^2 - \nabla^2 + m_X^2)X^{\rho} = -gm_X^2A^{\rho}. \tag{3}$$

Considering definitions of electric and magnetic fields, $E^i = F^{i0}$, $B^i = -\frac{1}{2}\epsilon^{ijk}F^{jk}$, taking advantage of Bianchi identity, and restoring c, $\hbar$, ε_0, and μ_0 to return to the international system of units, we obtained the Maxwell equations with the DP in the system:

$$\begin{cases} \nabla \cdot \mathbf{E} = -e\rho/\varepsilon_0 - g_m cX^0 \\ \nabla \times \mathbf{B} = \frac{\partial \mathbf{E}}{c^2\partial t} + \mu \mathbf{j}/d - g_m \mathbf{X} \\ \nabla \cdot \mathbf{B} = 0 \\ \nabla \times \mathbf{E} = -\frac{\partial \mathbf{B}}{\partial t} \\ \frac{\partial^2 X^{\sigma}}{c^2\partial^2 t^2} - \nabla^2 X^{\sigma} + m_X'^2 X^{\sigma} = -g_m A^{\sigma} \end{cases}, \tag{4}$$

where $\rho = (n - n_0)/d$; $\mathbf{j} = \mathbf{J}d$ are the linear current densities in graphene sheets: $g_m = gm_X'^2 \equiv g\frac{m_X^2c^2}{\hbar^2}$ and $m_X'^2 = \frac{m_X^2c^2}{\hbar^2}$.

Now, we introduced fluid dynamics in this study. The hydrodynamic equation of the carrier is as follows:

$$m_g n\frac{\partial \mathbf{v}}{\partial t} + m_g n(\mathbf{v}\cdot\nabla)\mathbf{v} = -en(\mathbf{E}_{\parallel} + \mathbf{v}\times\mathbf{B}) - \nabla P, \tag{5}$$

where e, n, $\mathbf{v}$ are carrier charge, 2D carrier density, and fluid velocity, respectively; $\mathbf{E}_{\parallel}$ is the projection of $\mathbf{E}$ in graphene sheets. In the above equation $m_g = \hbar k_F/v_F$ is the effective mass of carriers at the Fermi surface [32,33] and $P = \frac{\hbar v_F}{3\pi}(\pi n)^{3/2}$ ($\nabla P = \frac{\hbar v_F}{2}\sqrt{\pi n}\nabla n$) represents the carrier pressure in the graphene.

The continuity equation is

$$\frac{\partial n}{\partial t} + \nabla\cdot(n\mathbf{v}) = 0. \tag{6}$$

To linearize the above equations, we write $n = n_1 + n_0$, where n_1 is the density perturbations around the carrier equilibrium density n_0. Here we assumed that the perturbation is not large, implying $|n_1| \ll n_0$. The hydrodynamic equation and the continuity equation are converted to

$$\frac{\partial \mathbf{v}}{\partial t} = -\frac{e}{m_g}\mathbf{E}_{\parallel} - \frac{\pi\hbar^2}{2m_g^2}\nabla n_1, \tag{7}$$

$$\frac{\partial n_1}{\partial t} + n_0\nabla\cdot\mathbf{v} = 0. \tag{8}$$

Next, we assumed that the quantities, such as n_1, $\mathbf{v}$, X^{ρ}, $\mathbf{E}$, and $\mathbf{B}$, go as $e^{i\mathbf{q}\cdot\mathbf{r}-i\omega t}$. One can get modified Helmholtz equations for electric and magnetic fields for the structure, which becomes

$$\begin{aligned} \kappa^2\mathbf{E} &= i\frac{en_1}{d\varepsilon_0}\mathbf{q} + ig_m cX^0\mathbf{q} + i\frac{\omega\mu_0}{d}\mathbf{j} - i\omega g_m\mathbf{X}, \\ \kappa^2\mathbf{B} &= i\frac{\mu_0\mathbf{q}\times\mathbf{j}}{d} - ig_m\mathbf{q}\times\mathbf{X}, \end{aligned} \tag{9}$$

where $\kappa^2 = q^2 - \frac{\omega^2}{c^2}$. We returned to the ordinary Helmholtz equations for electric and magnetic fields provided $g_m = 0$.

However, one cannot use the above result directly, because we do not deduce the kinematic equation of DP. We first used

$$X^\rho = -\frac{g_m}{\kappa^2 + m_X'^2} A^\rho \tag{10}$$

to absorb the contribution of DP into 4D vector potential.

Substituting $\mathbf{E} = \mathrm{i}(\omega\mathbf{A} - cA^0\mathbf{q})$ and $\mathbf{B} = \mathrm{i}\mathbf{q} \times \mathbf{A}$ into Eq. (9), one finally gets

$$\begin{aligned} \lambda^2\mathbf{E} &= \mathrm{i}\frac{en_1}{d\varepsilon_0}\mathbf{q} + \mathrm{i}\frac{\omega\mu_0}{d}\mathbf{j}, \\ \lambda^2\mathbf{B} &= \mathrm{i}\frac{\mu_0\mathbf{q}\times\mathbf{j}}{d} = -\mathrm{i}\frac{en_0\mu_0}{d}\mathbf{q}\times\mathbf{v}, \end{aligned} \tag{11}$$

where we have set $\lambda^2 = \kappa^2 - \frac{g_m^2}{\kappa^2 + m_X'^2}$ and $\mathbf{j} = -en_0\mathbf{v}$.

The continuity equation and the hydrodynamic equation change to

$$\begin{aligned} \omega n_1 &= n_0\mathbf{q}\cdot\mathbf{v}, \\ -\mathrm{i}\omega\mathbf{v} &= \left(-\frac{e}{m_g}\mathbf{E} - \mathrm{i}n_1\frac{\pi\hbar^2}{2m_g^2}\mathbf{q}\right)_{\parallel}. \end{aligned} \tag{12}$$

Now, we focused on the mode in which $\mathbf{q}$ is parallel to graphene sheets for simplification, i.e., the mode propagates along graphene sheets. Thus, we have

$$\omega\left(1 + \frac{\omega_p^2}{c^2\lambda^2}\right)\mathbf{v} = \left(\frac{\pi\hbar^2}{2m_g^2} + \frac{\omega_p^2}{n_0\lambda^2}\right)n_1\mathbf{q}, \tag{13}$$

where n_0/d is the effective density of carriers, $\omega_p = \sqrt{\frac{e^2 n_0}{d\varepsilon_0 m_g}}$ refers the classic plasmon frequency of 3D gas. Combining with the continued equation of carrier, we finally obtain

$$\left(1 + \frac{\omega_p^2}{c^2\lambda^2}\right)\omega^2 = \left(\frac{v_F^2}{2} + \frac{\omega_p^2}{\lambda^2}\right)q^2. \tag{14}$$

In other words, one gets

$$\kappa^2(\kappa^2 + m_X'^2)(\omega^2 - \omega_p^2 - q^2v_F^2/2) = (\omega^2 - q^2v_F^2/2)g_m^2. \tag{15}$$

To clarify the above result, we introduce dimensionless quantities, $\omega_0 = \omega/\omega_p$, $q_0 = cq/\omega_p$, $m_0 \equiv m_X'\frac{c}{\omega_p} = \frac{m_X c^2}{\hbar\omega_p}$, $v_{F0} = v_F/c$. We finally obtain

$$\begin{aligned} &(\omega_0^2 - q_0^2)(\omega_0^2 - q_0^2 - m_0^2)(\omega_0^2 - 1 - q_0^2v_{F0}^2/2) \\ &\quad = (\omega_0^2 - q_0^2v_{F0}^2/2)g^2m_0^4. \end{aligned} \tag{16}$$

III. MODE DISPERSIONS

The above equation shows branch dispersions. For the sake of clarity, we first set $gm_0^2 = 0$. One can find three solutions of Eq. (16):

(1) $\omega_{ph0} = q_0$. This solution corresponds to photon branch.

(2) $\omega_{dp0}^2 = q_0^2 + m_0^2$. This solution corresponds to dark photon branch.

(3) $\omega_{pl0}^2 = 1 + q_0^2v_{F0}^2/2$. This solution corresponds to plasmon polariton branch. The term $q_0^2v_{F0}^2/2$ sources from the nonlocal effect [34].

Notably, two cases led to the decoupling between DP and ordinary matters. One is $g = 0$, which is a trivial case that there is no coupling between DP and photon. The other is $m_0 = 0$, implying that if DP is massless, there is no influence on photon and plasmon polariton dispersions. This conclusion agrees with other issues. For instance, authors in Ref. [6] found that one can remove the kinetic mixing through the redefinition of fields. We emphasized no momentum and energy gaps in dispersion curves, whether DP, photon, or plasmon.

Using Eq. (16), one can attribute the effect of dark photons to changes in the branch dispersions. We turned on g_0 and consider the effect of mixing between DP and photon. As a preliminary study, we first list dispersion relationships of photon, dark photon, and plasmon polariton, respectively, in Fig. 2, where we set $g = 0.01$ and $m_0 = 1.0$. We found that the correction to dispersion relationship of a dark photon is tiny and ignorable since $g \ll 1$. Due to the difficulty in explicitly detecting DP, the correction is irrelevant to our discussion, and we will not further investigate the dispersion relationship.

However, there are momentum gaps in photon and plasmon dispersions, as shown in Fig. 2, which was clarified by the inset. The momentum gaps are located in the vicinity $\omega_0 \sim q_0 \sim 1$, where photon and plasmon

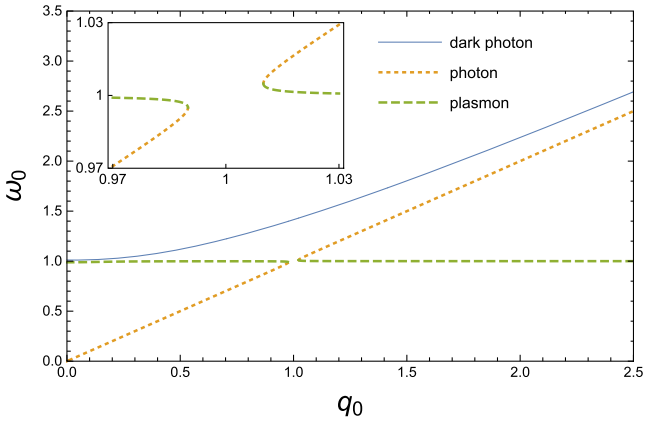

FIG. 2. Dispersion relations of dark photon, photon, and plasmon polariton. Here we set $g = 0.01$ and $m_0 = 1.0$. Dispersions of photon and plasmon polariton at the vicinity of $q_0 \sim 1$ are also shown in the inset.

polariton dispersions are very close. Figure 2 shows that there are intersection points of the photon dispersion curve and plasmon polariton one at the gap edges. Furthermore, as for the momentum gap of plasmon dispersion, there is a droop (an upturn) at the lower (upper) edge.

In the vicinity around matching point [35] where the photon dispersion and plasmon dispersion are the same, if there is not a dark photon, that is, $\omega_0 \sim q_0 \sim 1$, resonance absorption occurs, and photon and plasmon eventually evolve into dark photons, which leads to the result that neither photon nor plasmon can propagate in the structure. In this sense, one can consider the graphene cubic periodic structure as a producer of dark photons, especially around the matching point. Therefore, the momentum gap is always located in the vicinity of $q_0 \sim 1$. For the further research, with the constraint $w_2, q_2, m_2, g_2 \geq 0$, we consider the following function

$$f = (\omega_2 - q_2)(\omega_2 - q_2 - m_2)(\omega_2 - 1) - \omega_2 g_2 m_2^2, \tag{17}$$

which mimics Eq. (16) but ignores the unimportant term $q_0^2 v_{F0}^2/2$ since $v_{F0} = 1/300$, and the considering q_0 range is $q_0 \sim 1$. Since $f(\omega_2 = 0) = -(m_2 + q_2)q_2 < 0$ and $f(\omega_2 \to +\infty) \to +\infty$, there are always real solutions of ω_2 in the equation $f = 0$. Here, f is a cubic polynomial of ω_2, where three solutions correspond to DP, photon, and plasmon, respectively. The maximum of solutions, a real number, corresponds to DP. However, the other two solutions unlikely must be real numbers.

To clarify the statement we list the results of f vs ω_2 at $q_2 = 0.8, 1.0, 1.2$ in Fig. 3, where we set $g_2 = 0.01$ and $m_2 = 0.5$. The figure exhibits that for the equation $f = 0$, there are three positive real number solutions at cases $q_2 = 0.8$ and $q_2 = 1.2$, and only one real number solution exists at the case $q_2 = 1$, which corresponds to DP. Therefore, the case must have a momentum gap in photon and plasmon dispersions.

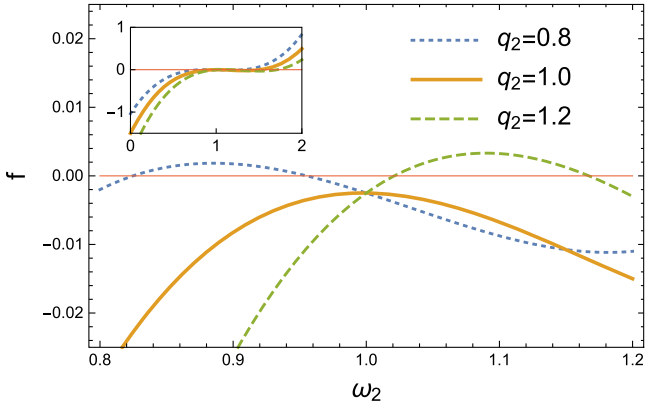

FIG. 3. f vs ω_2 at the resonance vicinity. Here we set $g_2 = 0.01$, $m_2 = 0.5$, and $q_2 = 0.8, 1.0$, and 1.2, respectively. The inset is an overall figure.

A more detailed study shows that provided $g_2 > 0$ and $m_2 > 0$, such a momentum gap in photon and/or plasmon dispersions always exists. Conversely, photon and plasmon dispersion behavior with $g_2 > 0$ and $m_2 > 0$ is significant different from that with $g_2 = 0$ or $m_2 = 0$.

Since the momentum gap is an universal phenomenon when there exists mixing between DP and ordinary matters, one can use the momentum gap to detect the presence or absence of dark photons in our Universe or to test whether the modified Maxwell equations are correct or wrong. Momentum gaps of photon and plasmon are the same. However, observing the plasmon momentum gap is more convenient since we are working in the graphene cubic structure.

Suppose $g_2 \ll 1$, $m_2 \sim 1$, and $g_2 m_2 \ll 1$, a simple discussion shows that $(q_2)_{\text{upper edge}} - (q_2)_{\text{lower edge}} \simeq 4\sqrt{g_2 m_2} + o(g_2^{3/2})$. The momentum gap always occurs at $q_0 \sim 1$, and we can obtain an approximate expression of the momentum gap as follows:

$$\Delta q_0 \simeq 2gm_0 = 2\frac{g m_X c^2}{\hbar \omega_p}, \tag{18a}$$

or in the form utilizing dimension quantities

$$\Delta q \lambda_X \simeq 4\pi g, \tag{18b}$$

where $\lambda_X = \frac{h}{m_X c}$ refers to the Compton wavelength of DP. This is an interesting result, because it combines the Compton wavelength of DP, the coupling between DP and photon, and the momentum gap of plasmon/photon in the graphene cubic structure.

In general, g is tiny, which leads to a tiny momentum gap of plasmon. However, since the gap always occurs in the vicinity of resonance absorption, $\omega \sim \omega_p$, it is not very difficult to detect the gap. The only limitation of the proposed detection is the fineness of the momentum interval of the detection instruments. Of course, we also need extremely low ambient temperature.

Suppose that $m_X \sim 0.1\ \text{meV}/c^2$, which means $\lambda_X \sim 1.24$ cm. If we also set $g \sim 10^{-5}$, then it is obtained that $\Delta q \sim 10^{-4}\ \text{cm}^{-1}$. Note that in general we also require $\hbar\omega_p > m_X c^2$, in other words, the classic plasmon frequency $f_p > 24$ GHz. Experimental requirements are not very stringent.

There are several literatures focused on the plasmon momentum (or plasmon wavelength) measurements based on graphene structures, such as Refs. [36–39]. Utilizing the scattering-type scanning near-field optical microscope, these references measured wavelength of graphene plasmon excited by focused infrared laser beam illuminating on graphene material and the tip of atomic force microscope, for instance, Ref. [37] obtained a plasmon dispersion relationship between frequency and wave vector in high

accuracy. However, since these jobs mainly focused on the plasmon in graphene planar structure, the plasmon in graphene periodic cubic structure need more studies. On the other hand, where there is momentum gap in plasmon dispersion is a completely new topic, and, to the best of our knowledge, there is little work on it.

IV. CONCLUSIONS

As a candidate for dark matter and a hypothetical particle needed in the extension of the standard model, dark photon is worth studying in depth. In the paper we proposed a cubic periodic structure made of graphene sheets. We discussed the modified Maxwell equations and the resulting hydrodynamics model in the system using the assumption that the dark photon exists in our Universe, which can kinetically mix with ordinary photon. The dispersion relationships of DP, photon, and plasmon in the system were obtained. We found that corrected plasmon/photon dispersion is significantly different from that without DP and kinetic mixing, that is, there is a gap in the momentum space. Our results showed a deep relationship between the momentum gap of photon/plasmon, the Compton wavelength of DP and the coupling constant of DP and photon.

The momentum gap occurs at the resonance absorption vicinity, $\omega = \omega_p$ and $q = \omega/c$, which implies that the detection is not difficult. One can, therefore, use the momentum gap to detect whether or not the DP exists in the Universe. For some detection strategies, one should always align the operating frequency of the detection instrument with the measured dark photon mass. However, the alignment is unnecessary for our strategy. Notice here that the cubic structure for graphene material is essential. This is because that the cubic periodic structure of graphene guarantees the existence of matching point [35]. As long as the momentum interval of the detection instruments is fine enough, it is possible to detect DP, despite its extremely small rest mass. Our study supplies an easy-to-realize platform to produce DP and detect effects induced by DP.

[1] A. Caputo, H. Liu, S. Mishra-Sharma, and J. T. Ruderman, Dark photon oscillations in our inhomogeneous universe, Phys. Rev. Lett. **125**, 221303 (2020).

[2] B. T. McAllister, A. Quiskamp, C. A. J. OHare, P. Altin, E. N. Ivanov, M. Goryachev, and M. E. Tobar, Limits on dark photons, scalars, and axion-electromagnetodynamics with the ORGAN experiment, Ann. Phys. (Amsterdam) **2023**, 220062 (2023).

[3] P. Adshead, K. D. Lozanov, and Z. J. Weiner, Dark photon dark matter from an oscillating dilaton, Phys. Rev. D **107**, 083519 (2023).

[4] N. Kitajima and F. Takahashi, Resonant production of dark photons from axions without a large coupling, Phys. Rev. D **107**, 123518 (2023).

[5] M. Fabbrichesi, E. Gabrielli, and G. Lanfranchi, *The Physics of the Dark Photon* (Springer, Cham, 2021).

[6] A. Caputo, A. J. Millar, C. A. J. O'Hare, and E. Vitagliano, Dark photon limits: A handbook, Phys. Rev. D **104**, 095029 (2021).

[7] H. An, S. Ge, W. Guo, X. Huang, J. Liu, and Z. Lu, Direct detection of dark photon dark matter using radio telescopes, Phys. Rev. Lett. **130**, 181001 (2023).

[8] LHCb Collaboration, Search for $A' \to \mu^+\mu^-$ decays, Phys. Rev. Lett. **124**, 041801 (2020).

[9] T. Ferber, C. Garcia-Cely, and K. Schmidt-Hoberg, Belle II sensitivity to longClived dark photons, Phys. Lett. B **833**, 137373 (2022).

[10] X. Chen, Z. Hu, Y. Wu, and K. Yi, Search for dark photon and dark matter signatures around electron-positron colliders, Phys. Lett. B **814**, 136076 (2021).

[11] M. Du, Z. Liu, and V. Q. Tran, Enhanced long-lived dark photon signals at the LHC, J. High Energy Phys. 05 (2020) 055.

[12] H. An, X. Chen, S. Ge, J. Liu, and Y. Luo, Searching for ultralight dark matter conversion in solar corona using LOFAR data, arXiv.2301.0362.

[13] C. Bartram, T. Braine, R. Cervantes, N. Crisosto *et al.*, Dark matter axion search using a josephson traveling wave parametric amplifier, Rev. Sci. Instrum. **94**, 044703 (2023).

[14] J. Liu, K. Dona, G. Hoshino, S. Knirck *et al.*, Broadband solenoidal haloscope for terahertz axion detection, Phys. Rev. Lett. **128**, 131801 (2022).

[15] L. Brouwer, S. Chaudhuri, H. M. Cho *et al.*, Projected sensitivity of DMRadio-m^3: A search for the QCD axion below 1 μeV, Phys. Rev. D **106**, 103008 (2022).

[16] K. M. Backes, D. A. Palken, S. Al Kenany, B. M. Brubaker *et al.*, A quantum enhanced search for dark matter axions, Nature (London) **590**, 238 (2021).

[17] A. Álvarez Melcón, S. A. Cuendis, J. Baier *et al.*, First results of the CAST-RADES haloscope search for axions at 34.67 μeV, J. High Energy Phys. 10 (2021) 075.

[18] H. Chang, J. Y. Chang, Y. C. Chang *et al.*, First results from the Taiwan axion search experiment with a haloscope at 19.6 μeV, Phys. Rev. Lett. **129**, 111802 (2022).

[19] XMASS Collaboration, Search for dark matter in the form of hidden photons and axion-like particles in the XMASS detector, Phys. Lett. B **787**, 153 (2018).

[20] J. Chiles, I. Charaev, R. Lasenby *et al.*, New constraints on dark photon dark matter with superconducting nanowire

detectors in an optical haloscope, Phys. Rev. Lett. **128**, 231802 (2022).
[21] N. Tomita, S. Oguri, Y. Inoue, M. Minowa, T. Nagasaki, J. Suzuki, and O. Tajima, Search for hidden-photon cold dark matter using a K-band cryogenic receiver, J. Cosmol. Astropart. Phys. 09 (2020) 012.
[22] FUNK Experiment Collaboration, Limits from the FUNK experiment on the mixing strength of hidden-photon dark matter in the visible and near-ultraviolet wavelength range, Phys. Rev. D **102**, 042001 (2020).
[23] B. Godfrey, J. A. Tyson, S. Hillbrand *et al.*, Search for dark photon dark matter: Dark E field radio pilot experiment, Phys. Rev. D **104**, 012013 (2021).
[24] P. Brun, L. Chevalier, and C. Flouzat, Direct searches for hidden-photon dark matter with the SHUKET experiment, Phys. Rev. Lett. **122**, 201801 (2019).
[25] A. V. Dixit, S. Chakram, K. He, A. Agrawal, R. K. Naik, D. I. Schuster, and A. Chou, Searching for dark matter with a superconducting qubit, Phys. Rev. Lett. **126**, 141302 (2021).
[26] R. Cervantes, G. Carosi, C. Hanretty *et al.*, Search for 70 μeV dark photon dark matter with a dielectrically loaded multiwavelength microwave cavity, Phys. Rev. Lett. **129**, 201301 (2022).
[27] DOSUE-RR Collaboration, Search for dark photon cold dark matter in the mass range $74-110\ \mu\mathrm{eV}/c^2$ with a cryogenic millimeter-wave receiver, Phys. Rev. Lett. **130**, 071805 (2023).
[28] H. An, F. P. Huang, J. Liu, and W. Xue, Radio-frequency dark photon dark matter across the sun, Phys. Rev. Lett. **126**, 181102 (2021).
[29] G. B. Gelmini, A. J. Millar, V. Takhistov, and E. Vitagliano, Probing dark photons with plasma haloscopes, Phys. Rev. D **102**, 043003 (2020).
[30] M. Lawson, A. J. Millar, M. Pancaldi, E. Vitagliano, and F. Wilczek, Tunable axion plasma haloscopes, Phys. Rev. Lett. **123**, 141802 (2019).
[31] A. J. Millar, S. M. Anlage, R. Balafendiev *et al.*, Searching for dark matter with plasma haloscopes, Phys. Rev. D **107**, 055013 (2023).
[32] A. J. Chaves, N. M. R. Peres, G. Smirnov, and N. A. Mortensen, Hydrodynamic model approach to the formation of plasmonic wakes in graphene, Phys. Rev. B **96**, 195438 (2017).
[33] D. Liu, X. Hua, D. Sun, X. Jiang, and X. Zhao, Axion-plasmon-polariton hybridization in a graphene periodic structure, J. High Energy Phys. 11 (2022) 052.
[34] X. Hua, D. Sun, X. Zhang, L. Wang, D. Liu, and N. Ma, Modified dispersion for graphene plasmon polariton in hydrodynamic model without potential notation, Solid State Commun. **369**, 115199 (2023).
[35] L. Zhang, L. Wang, D. Liu, X. Jiang, Y. He, and Ning Ma, Plasmon polaritons in 3D graphene periodic structure, Electromagnetics **42**, 210 (2022).
[36] J. Chen, M. Badioli, P. Alonso-Gonzlez *et al.*, Optical nano-imaging of gate-tuneable graphene plasmons, Nature (London) **487**, 77 (2022).
[37] H. Hu, R. Yu, and H. Teng, Active control of micrometer plasmon propagation in suspended graphene, Nat. Commun. **13**, 1465 (2022).
[38] Q. Xu, T. Ma, M. Danesh *et al.*, Effects of edge on graphene plasmons as revealed by infrared nanoimaging, Light Sci. Appl. **6**, e16204 (2017).
[39] L. Ju, B. Geng, J. Horng *et al.*, Graphene plasmonics for tunable terahertz metamaterials, Nat. Nanotechnol. **6**, 630 (2011).